Research article

Evaluation of SARS-CoV-2 inhibition of some compounds in*CYMBOPOGON CITRATUS* oil combining docking and molecular dynamics simulations

Bui Thi Phuong Thuy[1], Vo Duy Nhan[2], Nguyen Minh Quang[3], Nguyen Thanh Duoc[4], Pham Van Tat[5*]

[1]Faculty of Basic Sciences, Van Lang University, 45 Nguyen Khac Nhu, Co Giang, District 1, Ho Chi Minh City 70000, Viet Nam

[2]Faculty of Pharmacy, Nam Can Tho University, 168 Nguyen Van Cu, Ninh Kieu, Can Tho 94000, Viet Nam

[3]Faculty of Chemical Engineering, Industrial University of Ho Chi Minh City, 12 Nguyen Van Bao, Go Vap, Ho Chi Minh City 70000, Viet Nam

[4]Faculty of Pharmacy, Hong Bang International University, 3 Hoang Viet, Tan Binh, Ho Chi Minh City 70000, Viet Nam

[5]Faculty of Health Sciences, Hoa Sen University, 8 Nguyen Van Trang, District 1, Ho Chi Minh City 70000, Viet Nam

Abstract

The visual screening and simulation methods were used to evaluate the inhibitory ability of 34 compounds in *Cymbopogon citratus* oil against SARS-CoV-2. We chose the best compound, SC22, with a DS of -12.80 Kcal. mol^{-1} with a distance RMSD of 0.23. This was the most effective compound at inhibiting the viral protein 6LU7. For the protein ACE2 or an endemic host receptor, the docking ability of **SC**22 showed DS = -13.13 Kcal.mol^{-1} and RMSD = 1.32 Å; **SC**10 docked in DS = -12.79 Kcal.mol^{-1} and RMSD = 0.91 Å; **SC**11 gave the docking values DS = -12.77 Kcal.mol^{-1} and RMSD = 1.15 Å. **SC**26 showed DS = -12.76 Kcal.mol^{-1} and RMSD = 1.44 Å; **SC**20 showed DS = -12.68 Kcal.mol^{-1} and RMSD = 1.22 Å; the *Cymbopogon citratus* oil involved the potential compounds for contributing to drug development. The compounds SC10, SC11, SC20, SC22 also tested and refined the druglikeness properties. The compound SC22 gives many druglikeness properties and is easy to carry out drug synthesis.

Keywords. *Cymbopogon citratus* Oil, SARS-CoV-2, protein 6LU7, protein ACE2, Potential drugs.

1. INTRODUCTION

In the twenty-first century, a pandemic of diseases emerged, including chronic noncommunicable diseases such as diabetes, blood pressure, heart disease, gout, obesity, osteoarthritis, and disaster; infectious diseases such as seasonal flu, diphtheria, and tuberculosis. Furthermore, unhealthy lifestyles, a lack of nutrition, excess toxins, sedentary behavior, and a lack of sleep all contribute to an increase in cases and mortality. In 2019 and 2020, the SARS-CoV-2 pandemic broke out and spread to more than 200 countries and territories, including Vietnam. According to WHO reports, there were 31.1 million cases and 944 deaths worldwide on 2020. Many countries, including Russia, the United Kingdom, France, the United States, and Vietnam, are researching and developing a SARS-CoV-2 vaccine. COVID-19, caused by SARS-coronavirus-2 (SARS-CoV-2), has caused a worldwide pandemic, affecting hundreds of millions of people. Dan Zhang *et al.* provided insight into the clinical applications and basic mechanisms of the proposed CPM against COVID-19 virus to share Chinese clinical practices and provide research in the fierce battle against COVID-19 virus.[1] Several drugs, including favipiravir, remdesivir, ritonavir, lopinavir, and chloroquine, have been studied for their ability to inhibit the SARS-CoV-2 virus.[2] Furthermore, natural compounds such as *Allium sativum* L. have been proposed to inhibit the virus SARS-CoV-2,[3] *Melaleuca* L. oil,[4] Curcumin compounds,[5] flavonoid derivatives.[6] Folk remedies show that *Cymbopogon citratus* oil contains many compounds

with antioxidant, antibacterial, antifungal, anti-inflammatory, anti-proliferative, and inhibitory properties, according to traditional medicine sources. Cancer prevention and immune system bolstering.[7,8] As demonstrated by Neetu Jain *et al*., lemongrass has strong antiseptic properties and treats staph infections more effectively than antibiotics.[9]

The SARS-CoV-2 virus is a new coronavirus line with a genome that shares many similarities with the Mers-CoV virus and the SARS-CoV-1 virus.[10] There are two viral therapy methods: viral receptor suppression or viral protein suppression against SARS-CoV-2 and ACE2 proteins or (Angiotensin-convert enzyme II), with 6LU7 being the main protein. Each protein has an active site, and the compounds may occupy a position in the ACE2 active site more strongly than viral binding to ACE2, indicating that competition is being inhibited. This strategy can be used to investigate the virus's "host" receptor.[10] When the active site binds to the active substance, one of two things happens: the virus is either inhibited or activated and grows faster. A molecule can bind to the active site of protein 6LU7, inhibiting viral activity, as suggested by Ai Nhung *et al*.[3,4] The use of docking simulation and quantum chemistry will significantly accelerate the drug screening process. Drug development is becoming a new approach both at home and abroad. As a result, the development of research directions for these methods is critical.[8] Docking simulations have been widely used for preclinical evaluation of potential drugs efficacy in antimicrobial, antifungal, or antiviral therapy.

There are several explanations for the earlier effects in the treatment of SARS-COV-2 patients in Vietnam. Many of the drugs and regimens used by Vietnamese doctors to treat patients with respiratory tract infections are also used to treat HIV patients. Another treatment that has been shown to work is the use of chloroquine and an antibiotic to treat the SARS-CoV-2 virus. All of these drugs, however, are still in the research and development stage. Meanwhile, many different drugs from the antibacterial, antifungal, and antiviral groups are being considered and studied. The development of a new drug and inhibitory mechanism for SARS-COV-2 still necessitates extensive research.

The purpose of this study was to assess the ability of the components in Cymbopogon citratus essential oil to inhibit SARS-CoV-2 protein as well as bind to the ACE2 protein - the host receptor. Dynamic and docking simulation techniques were used to assess the inhibitory potential of components in Cymbopogon citratus essential oil against SARS-CoV-2 (MD). In addition, in this paper, we combine with virtual screening techniques to refine the compound to produce a drug-like compound that is simple to synthesize via pharmacochemistry. This is the direction in which researchers are looking for potential drugs that inhibit the SARS-CoV-2 protein, which is desperately needed.

2. MATERIALS AND METHODS

2.1. Experimental data

Experimental database of essential oil compounds, including 34 compounds from *Cymbopogon citratus* essential oil (SC1-SC34), with structural and reference content data from the same source as Neetu Jain *et al*.[9] SC1: 3-Hexen-1-ol, 0.08 %; SC2: α-Pinene, 0.05 %; SC3: Methyl heptenone, 0.47 %; SC4: Octanal, 0.11 %; SC5: δ-3-Carene, 0.05 %; SC6: Limonene, 1.70 %; SC7: *trans*-β-Ocimene, 0.07 %; SC8: Caryophyllene oxide, 1.07 %; SC9: Propyl amyl ketone, 1.88 %; SC10: *trans*-linalool oxide, 0.04 %; SC11: Linalool, 0.31 %; SC12: *cis*-Verbenol, 0.05 %; SC13: *cis*-Limonene oxide, 0.11%; SC14: γ-Geranial, 0.24 %; SC15: *trans*-Chrysanthemol, 0.32 %; SC16: Isogeranial, 2.25 %; SC17: Humulene epoxide II, 0.10 %; SC18: Lilac aldehyde, 0.60 %; SC19: Decanal, 0.16 %; SC20: geranial, 48.26 %; SC21: Neral, 39.85 %; SC22: Epoxy-Linalool oxide, 0.22 %; SC23: 2-Hexenyl laurate, 0.17 %; SC24: Eugenol, 0.08 %; SC25: Yomogi alcohol, 0.16 %; SC26: Geranyl acetate, 0.42 %; SC27: trans-Caryophyllene, 0.32 %; SC28: Chrysanthenone, 0.10 %; SC29: Dihydroisocary-ophyllene epoxide, 0.02 %; SC30: α-Humulene, 0.06 %; SC31: Cuparene, 0.07 %; SC32: γ-Muurolene, 0.52 %; SC33: *cis*-γ-Bisabolene, 0.07 %; SC34: Geranyl Butyrate, 0.02 %.

2.2. Docking simulation

Docking simulation: The ACE2 protein, or viral host receptor, and the 6lu7 protein, or SARS-CoV-2 protein, are loaded from the Protein data bank (PDB) system using MOE 2015.10. The protein then decomposes into water molecules, selects the situation area, and saves it as a*.pdb file. The site was chosen using the location Finder technique, so that essential amino acids could be discovered in order to investigate ligand binding.[3,11] Following the processes outlined below, we used the Site Finder method to locate a suitable location for our business: providing a receptor molecule for the system; hydrogens and protonation states are not required because the Site Finder uses only heavy atoms. The Site Finder technique brings up the Site Finder panel. Finally, the Atoms section of the panel is where you

configure your options. The force field MMFF94x was used to structure 34 compounds in *Cymbopogon citratus* essential oil[3,4] and then held * .mdb to prepare for the docking assembly simulation process. The docking simulation parameters were set to a maximum of 1000 repetitions, 200 fragments, and 5 profiles for analysis. The docking model obtained includes docking score (DS < -3.2 Kcal.mol^{-1}), (RMSD < 2.0 Å), and types of interactions such as van der Waals interaction, H-acceptor, H-donor, H-pi, cation-pi, and pi-pi.[3] Molecular dynamics simulations with 20000 ps epochs and CHARM-27 force fields were used to assess the ligand ability to bind to the active sites on the 6LU7 protein of SARS-CoV-2 and ACE2. To simulate interactions with the protein receptors ACE2 and 6LU7, the compound SC22 with the highest inhibitory potential was used. The molecular mechanics method also calculates the properties logP, polarity, and molecular volume.[12]

3. RESULTS AND DISCUSSION

3.1. Protein and ligand preparation

The primary source of 3D biomolecular structure data, principally established by employing single-crystal X-ray data, was used to create 3D protein structures for SARS-CoV-2 and ACE2.

We looked at crystal structures of non-amino acid bonded forms. They can be calculated using heavy atom positions. Furthermore, due to the high flexibility of hydrogen atoms, th e binding order is based on their ability to bind. As a result, the ligand's protonation state must be verified and, if necessary, corrected. We then went on to prepare protein receptors from crystal structures of protein, which included the steps listed below:

- Import protein structures from the PDB6LU7 and PDBACE2 databases.

- Examine protein geometry, structure, and electron density by varying temperature factors in order to test and evaluate the PDB data quality.

- Investigate the alternative structure data.

- Using the homology model and rotamer disCoVery, replace the missing protein fractions.

- Examine and investigate the repair of bonding types in the co-factor and ligand, as well as the deletion of unbound water molecules.

- Add hydrogen to the unsaturated bonding sites, then optimize the site.

- Install tethers and restraints.

- Continue to reduce the structure's final energy.

- These procedures have resulted in the creation of automated bio-protein molecular structures.

- We prepare 3D small molecular structures

(ligands) primarily by doing the following:

- Draw the molecular structure of a ligand or obtain data on small molecules from an external data source.

- Molecular testing in 2D and 3D; atomic bonding errors are correctable.

- The protonation and tautomeric states are decided upon.

- The stereoscopic chemical structure is also edited if required.

- The molecule is charged with a partial charge that has been calculated.

- Any geometrical limits (distance, angle, dihedral) are defined as well.

- Next, using an appropriate force field MMFF94, minimize energy.

This procedure yields a prepared and miniaturized 3D small molecular structure (ligand). A small molecular database can also be used to copy 3D structures.

In section 2.1, thirty-four compounds from *Cymbopogon citratus* were structurally reconstructed using ChemOffice 2018; docking simulations were run using a database of optimized small molecules. The active sites in the proteins ACE2 and 6LU7 (in Figure 1) are determined, and the distance between the ligands, including amino acids, is determined by hydrogen bonds, *pi* bonds, and van der Waals energy bonds.

3.2. Simulation results

The docking scores (DS) and RMSD (root-mean-square deviation) between the ligand and protein were presented in table 1 for the 34 molecules in lemongrass essential oil (SC1 to SC34).

The DS of the ligand and 6LU7 protein ranges from -12.8 to -8.21 kcal.mol^{-1}; the DS of the ligand and ACE2 protein ranges from -13.3 to -7.98 kcal.mol^{-1}. Complexes have an RMSD value less than 2 Å, which is consistent with the excellent distance criteria in complexes, as depicted in Table 1 and figure 1. The mean DS value in the models of ligand-6LU7 complex and ligand-ACE2 was -9.94 and -9.97 kcal.mol^{-1}, respectively. It was computed using the average DS value. For the inhibitory capacity 6LU7: The five compounds with the highest docking scores were SC22, SC10, SC11, SC26, and SC20, with docking models shown in figure 1: SC22 with DS = -12.80 kcal.mol^{-1} and distance RMSD = 0.23 Å; SC22 formed three hydrogen interactions with Leu 141, Cys 145, and Gly 143; a strong affinity for amino acids, including Met 165, Asn 142, His 163, His 41, Glu 166, His 164, Ser 144, Leu 27, Thr 25, Met 49, Thr 26. They are essential amino acids in the active

site region of the 6LU7 protein.

Table 1: The docking results DS, RMSD between ligands on ACE2 and 6LU7 protein

Compound	DS-6LU7 (Kcal.mol^{-1})	RMSD-6LU7 (Å)	Compound	DS-ACE2 (Kcal.mol^{-1})	RMSD-ACE2 (Å)	LogP
SC22	-12.80	0.23	SC22	-13.13	1.32	1.88
SC10	-11.93	0.52	SC10	-12.79	0.91	1.66
SC11	-11.82	0.54	SC11	-12.77	1.15	2.08
SC26	-11.73	0.55	SC26	-12.76	1.44	3.48
SC20	-11.54	0.58	SC20	-12.68	1.22	2.81
SC34	-10.44	0.61	SC34	-10.91	0.97	4.17
SC21	-10.14	0.61	SC21	-10.90	1.51	2.81
SC19	-9.93	0.63	SC24	-10.90	1.27	2.97
SC18	-9.87	0.64	SC4	-10.86	1.35	1.91
SC24	-9.85	0.64	SC1	-10.85	1.00	2.03
SC4	-9.82	0.64	SC14	-10.84	1.28	1.22
SC17	-9.80	0.66	SC25	-10.84	0.67	2.95
SC16	-9.75	0.66	SC18	-10.84	1.17	2.86
SC29	-9.67	0.66	SC19	-9.83	0.95	3.03
SC28	-9.65	0.67	SC28	-9.82	2.06	2.08
SC1	-9.60	0.67	SC17	-9.75	2.12	0.9
SC25	-9.58	0.70	SC16	-9.75	1.41	2.0
SC15	-9.54	0.71	SC29	-9.73	0.90	1.90
SC14	-9.47	0.74	SC15	-9.73	1.34	2.79
SC23	-9.47	0.76	SC23	-9.73	0.79	3.70
SC33	-9.21	0.79	SC33	-9.73	1.41	5.72
SC8	-9.21	0.79	SC8	-9.73	0.79	3.03
SC30	-9.17	0.79	SC30	-8.71	1.43	4.76
SC27	-9.17	0.81	SC27	-8.51	2.00	4.99
SC32	-9.05	0.86	SC32	-8.50	1.70	5.23
SC13	-9.02	0.89	SC13	-8.42	0.96	2.05
SC3	-9.01	0.90	SC3	-8.41	2.08	1.13
SC9	-8.93	0.90	SC9	-8.40	0.99	2.43
SC7	-8.86	0.91	SC7	-8.39	1.08	4.09
SC12	-8.83	0.92	SC12	-8.25	1.52	1.94
SC6	-8.80	0.93	SC6	-8.24	0.55	7.57
SC2	-8.69	0.93	SC2	-8.11	1.18	3.88
SC31	-8.63	0.94	SC31	-8.04	0.66	5.01
SC5	-8.21	0.95	SC5	-7.98	2.77	4.18

The mean DS value in the models of ligand-6LU7 complex and ligand-ACE2 was -9.94 and -9.97 kcal.mol^{-1}, respectively. It was computed using the average DS value. For the inhibitory capacity 6LU7, five compounds with the highest docking scores were SC22, SC10, SC11, SC26, and SC20. By using the docking models shown in figure 1, SC22 with DS = -12.80 kcal.mol^{-1} and distance RMSD = 0.23Å. SC22 formed three hydrogen interactions with Leu 141, Cys 145, and Gly 143; a strong affinity for amino acids, including Met 165, Asn 142, His 163, His 41, Glu 166, His 164, Ser 144, Leu 27, Thr 25, Met 49, Thr 26. They are essential amino acids in the active site region of the 6LU7 protein.
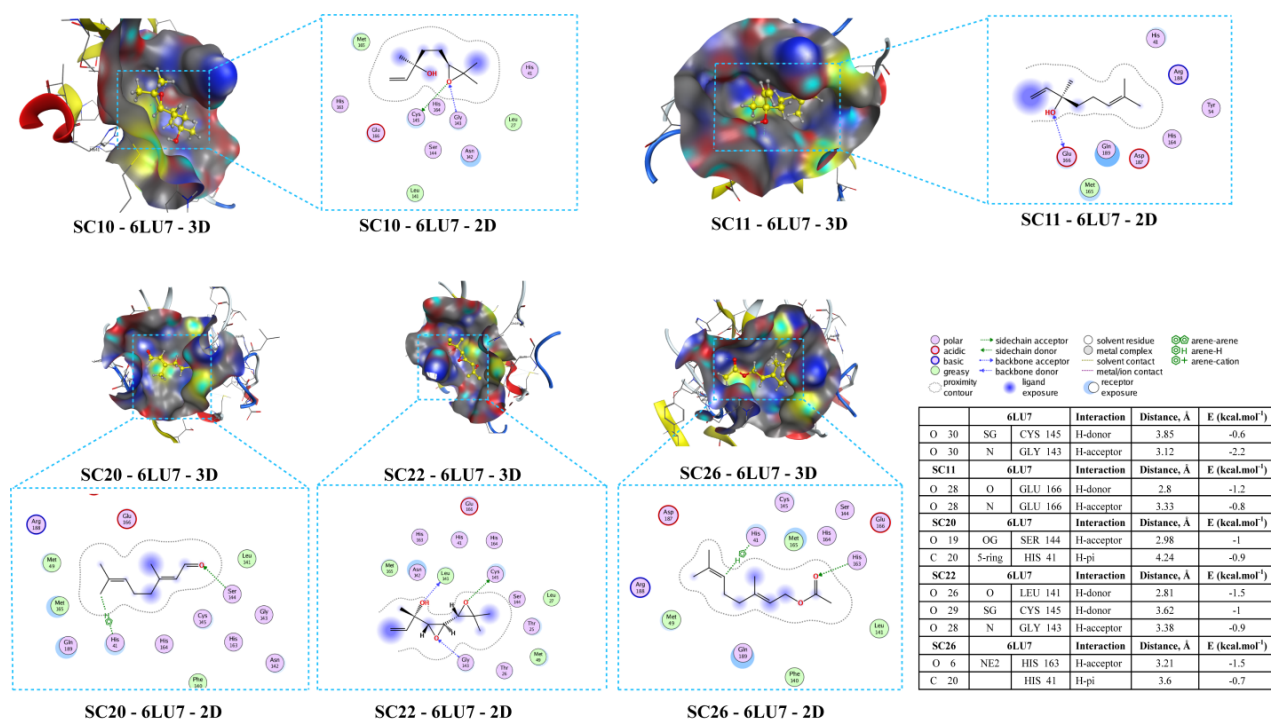
SC10 - 6LU7 - 3D   SC10 - 6LU7 - 2D   SC11 - 6LU7 - 3D   SC11 - 6LU7 - 2D

SC20 - 6LU7 - 3D   SC22 - 6LU7 - 3D   SC26 - 6LU7 - 3D

SC20 - 6LU7 - 2D   SC22 - 6LU7 - 2D   SC26 - 6LU7 - 2D

	6LU7		Interaction	Distance, Å	E (kcal.mol⁻¹)
O 30	SG	CYS 145	H-donor	3.85	-0.6
O 30	N	GLY 143	H-acceptor	3.12	-2.2
SC11	**6LU7**		**Interaction**	**Distance, Å**	**E (kcal.mol⁻¹)**
O 28	O	GLU 166	H-donor	2.8	-1.2
O 28	N	GLU 166	H-acceptor	3.33	-0.8
SC20	**6LU7**		**Interaction**	**Distance, Å**	**E (kcal.mol⁻¹)**
O 19	OG	SER 144	H-acceptor	2.98	-1
C 20	5-ring	HIS 41	H-pi	4.24	-0.9
SC22	**6LU7**		**Interaction**	**Distance, Å**	**E (kcal.mol⁻¹)**
O 26	O	LEU 141	H-donor	2.81	-1.5
O 29	SG	CYS 145	H-donor	3.62	-1
O 28	N	GLY 143	H-acceptor	3.38	-0.9
SC26	**6LU7**		**Interaction**	**Distance, Å**	**E (kcal.mol⁻¹)**
O 6	NE2	HIS 163	H-acceptor	3.21	-1.5
C 20		HIS 41	H-pi	3.6	-0.7

Figure 1: The docking results for compounds SC10, SC11, SC20, SC22, and SC26 on the 6LU7 protein

The SC26-6LU7 complex is drawn by two hydrogen interactions with His 41 and His 163, as well as van der Waals interactions with amino acids like Asp 187, Arg 188, Met 49, Gln 189, Phe 140, Leu 141, Glu 166, Ser 144, His 164, Met 165, and Cys 145, as shown in figure 1. The SC20-6LU7 complex is drawn by two hydrogen interactions with His 41 and Ser 144, van der Waals interactions with amino acids such as Glu 166, Asp 187, Arg 188, Met 49, Met 165, Gln 189, His 164, Faction 140, Asn 142, His 163, Cys 145, Gly 143, as seen in figure 1.

Table 1 shows that the SC22 compound was remarkably flexible and strongly bound to the receptor amino acids after analyzing the complexes of ligand-6LU7 protein. Table 1 shows the docking model between ligand and ACE2 protein and the five complexes with the strongest binding: SC22, SC10, SC11, SC26, and SC20. SC22 has a DS = -13.13 Kcal.mol-1 and RMSD = 1.32 Å; the SC22-ACE2 complex has two hydrogen interactions with Gln 101 and Asn 103, as well as van der Waals interactions with Gln 81, Gln 98, Leu 85, His 195, Asn 194, Ala 193, and Gln 102. SC10 docked with DS = -12.79 kcal.mol⁻¹ and RMSD = 0.91 Å, as given in figure 2.

SC10 inhibited ACE2 protein interactions via two stable hydrogen bonds with Gln 101 and Asn 103. Figure 2 depicts van der Waals interactions between SC10 and ACE2 with amino acids such as Gln 102, Gln 98, Leu 85, Asn 194, Ala 193, His 195, and Gln 81. SC11 docking values were DS = -12.77 Kcal.mol⁻¹ and RMSD = 1.15 Å; the SC11 compound inhibits the ACE2 protein with two stable hydrogen bonds; the flexible OH group is SC11 and Gln 101 and Asn 103. Van der Waals interactions are formed by amino acids such as Gln 102, Gln 98, His 195, Asn 194, Tyr 196, and Gln 81. SC26 had DS = -12.76 kcal.mol and RMSD = 1.44 Å, as shown in figure 2.

The compound SC26 with the ACE2 protein is formed by two strong hydrogen bonds between the carbonyl group SC26 and the Lys 94 and Gln 98. The association of SC26 and amino acids such as Leu 95, Ala 99, Val 209, Glu 208, Gly 205, Tyr 196, and Gln 102 elucidates van der Waals interactions. SC20 exhibited DS = -12.68 Kcal.mol⁻¹ and RMSD = 1.22 Å, as shown in figure 2; the SC20 compound is bound to ACE2 proteins via two stable hydrogen bonds formed between the oxygen group carbonyl group and the Lys 94 and Gln 98. Van der Waals interactions are generated by amino acids such as Lys 562, Ala 396, Asp 206, Val 209, Pro 565, Asn 210, Val 212, Leu 95, and Glu 208, as indicated in figure 2.

The ability to inhibit the ACE2 protein of SC22 is best represented in the diagram, which includes 34 lemongrass essential oil substances with negative DS energy.
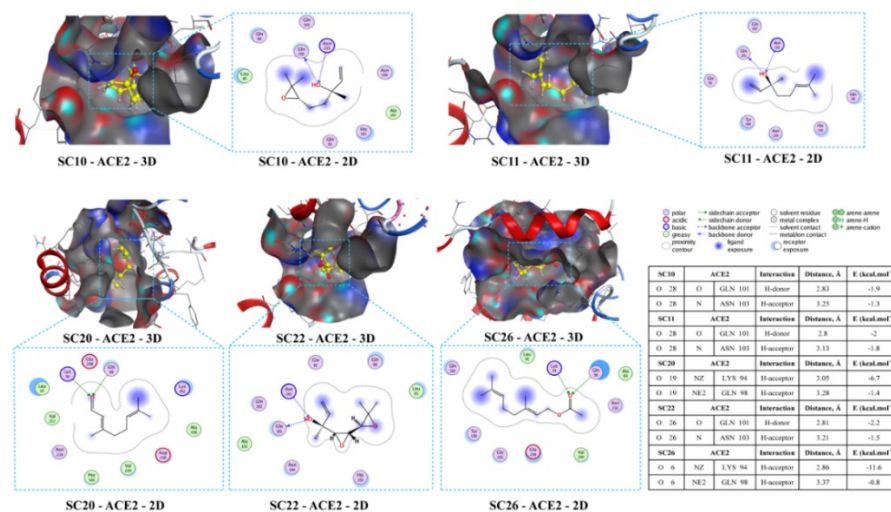
SC10	ACE2		Interaction	Distance, Å	E (kcal.mol⁻¹)
O 28	O	GLN 101	H-donor	2.83	-1.9
O 28	N	ASN 103	H-acceptor	3.25	-1.3
SC11	**ACE2**		**Interaction**	**Distance, Å**	**E (kcal.mol⁻¹)**
O 28	O	GLN 101	H-donor	2.8	-2
O 28	N	ASN 103	H-acceptor	3.13	-1.8
SC20	**ACE2**		**Interaction**	**Distance, Å**	**E (kcal.mol⁻¹)**
O 19	NZ	LYS 94	H-acceptor	3.05	-6.7
O 19	NE2	GLN 98	H-acceptor	3.28	-1.4
SC22	**ACE2**		**Interaction**	**Distance, Å**	**E (kcal.mol⁻¹)**
O 26	O	GLN 101	H-donor	2.81	-2.2
O 26	N	ASN 103	H-acceptor	3.21	-1.5
SC26	**ACE2**		**Interaction**	**Distance, Å**	**E (kcal.mol⁻¹)**
O 6	NZ	LYS 94	H-acceptor	2.86	-11.6
O 6	NE2	GLN 98	H-acceptor	3.37	-0.8

Figure 2: SC10, SC11, SC20, SC22, SC26 with ACE2 protein

SC10: *trans*-linalool oxide, 0.04 percent; SC11: Linalool, 0.31 percent; SC20: geranial, 48.26 percent; SC22: Epoxy-Linalool oxide, 0.22 percent; and SC26: geranyl acetate, 0.42 percent are the top five inhibitory compounds. The total content of the essential oil compounds is 49.25 percent. The citral, also known as journal, is the main ingredient in lemongrass essential oil, and it is responsible for the main scent of lemongrass plants. These are antibacterial and antifungal compounds found in tea tree oil, lemongrass, lavender, and orange essential oil.[4]

Dock Score and Rating Score were assigned to the target binding ability of the studied compound SC22 and used as parameters for docking result analysis. The binding scores of the compounds studied are shown in table 1, where ligand-protein interactions are ranked based on the Dock and Rank scores, respectively. Based on the binding results, it was discovered that compound **SC**22 formed binding and non-binding interactions at the receptor's binding pocket, implying that the compounds have more favorable ligand-protein interaction energies than the remaining substances at the binding site, and the suit of this compound with the lowest energy was chosen for the next steps.
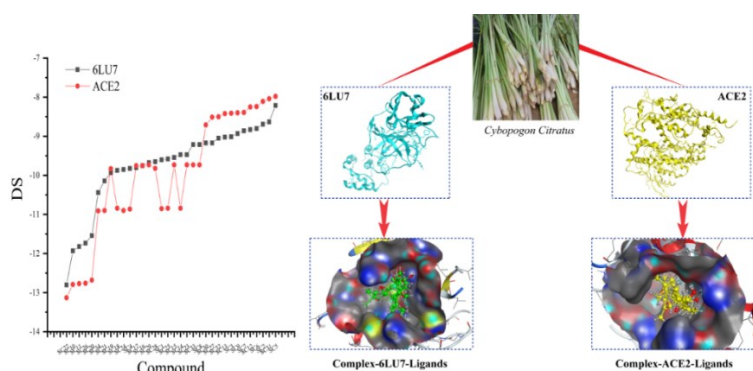
Figure 3: Homogenous inhibitory interaction of compounds in lemongrass with SARS-CoV-2 and competitive inhibition with the viral host or protein ACE2

The logP values for 34 compounds in lemongrass are calculated from the quantum chemistry calculation, as shown in table 1. The water solubility or logP of SC22, SC10, SC11, SC26, SC20 compounds are 1.88, 1.66, 2.08, 3.48, and 2.81 respectively (see table 1, figure 3). These solubility data have shown good water solubility of most compounds.[13] The compounds in lemongrass have small molecular volumes, logP < 5, molecular mass M < 500 Da, total hydrogen interactions H-donor and H-acceptor < 5, adapted to Lipinski's standard of pre-screening.[13]

The results showed that 34 compounds in lemongrass have a strong affinity for the amino acids of the active region of the protein ACE2 and protein 6LU7, as seen in figure 3. The ability of synergistic interaction to both inhibit the virus's receptors and "hit" directly on the virus of lemongrass compounds

is suitable. The above evidence shows potential in studies using lemongrass essential oil to prevent SARS-CoV-2 for further experimental investigations. The first step of simulation research shows the use of

vital oil therapy with a sufficient amount of each substance in insufficient red dosage, but the overall effect on many aspects prevents the virus from attacking the body.
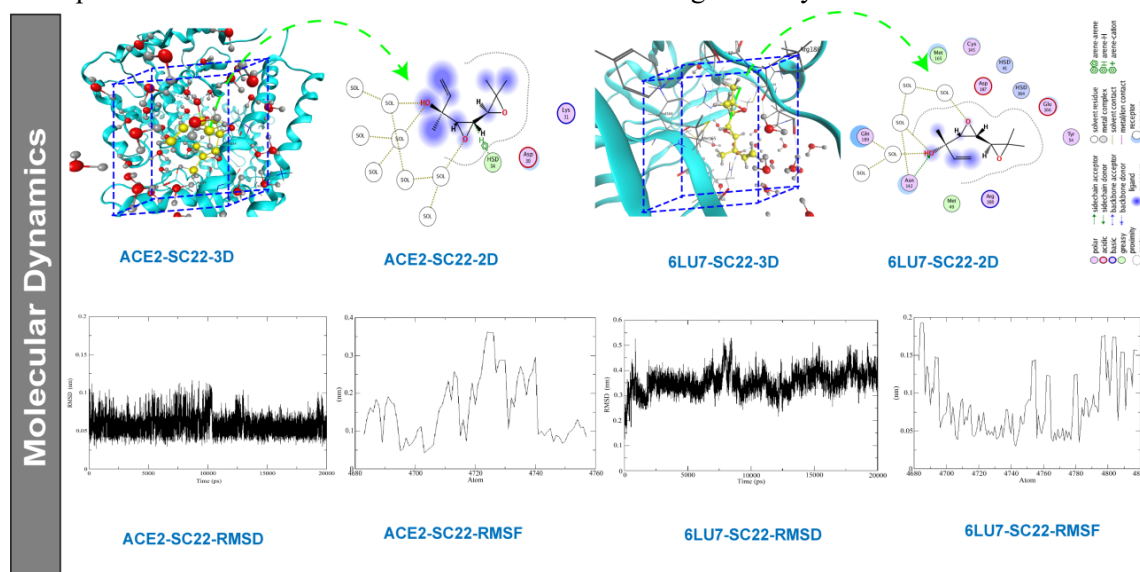

Figure 4: The changes RMSD and RMSF vs. simulation time (20,000 ps) calculated on the complexes SC22 with protein receptors ACE2 and 6LU7 in MD process

The MD simulations were conducted to demonstrate the binding stability of the SC22 inhibitor in the primary protease of SRAS-CoV-2 and the ACE2 host receptor. The MD models of SC22 compound with ACE2 and 6LU7 proteins are built. The RMSD value of the SC22-ACE2 complex is 0.025-0.12 nm, and its RMSF is 0.15-0.35 nm, as shown in Figure 4; the RMSD value of the SC22-6LU7 complex is 0.025-0.18 nm, and its RMSF is 0.1-0.3 nm. The MD simulation results also show that SC22 has a strong interaction with the ACE2 protein. As illustrated in figure 4, SC22 compound is strongly bound to Lys 31, Asp 30, Hsd 34, and sols in the binding cavity. Furthermore, SC22 has a high affinity for the 6LU7 protein. Interactions with binding amino acids Met 165, Cys 145, Hsd 41, Asp 187, Hsd 164, Glu 166, Tyr 54, Arg 188, Met 49, particularly Asn 142 and Gln 189, and Sols in the active site area are depicted. Thus, docking and MD simulation techniques have demonstrated the active potential of SC22 compound.

The molecular dynamic simulation results showed that SC22: Epoxy-Linalool oxide compound, which accounts for 0.22 % of citronella essential oil content, has good binding ability with both ACE2 and PDB6LU7 protein. This compound exhibits the most negative coupling docking score and creates stable interactions with the active region on proteins ACE2
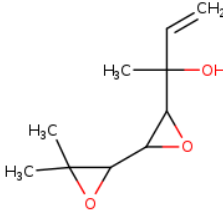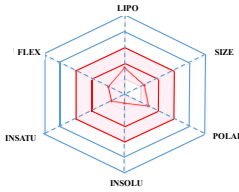
and PDB6LU7. A previous study that used MD simulation and docking simulation techniques indicated that parameters of potential inhibitors in *Cymbopogon citratus* essential oil for the proteins ACE2 and 6LU7 were in good agreement with the ones obtained from docking and MD models, such as DS < -3,2 kcal.mol^{-1}.[4,5] Moreover, RMSD values < 4 nm, RMSF < 4 nm[5,11] are consistent with the standard rule Linpiski. This also responds to the rule logP < 5, Mass < 500 DVC, H-acceptor and H-donor < 5.[13]

3.3. Refining the druglikeness properties

The investigated compounds were first virtual screened using Lipiskin rule. This rule will aid in the initial search for substances that have drug-like activity. Hydrogen bonding and the number of groups that accept hydrogen bonds are used to evaluate the molecule's bond groups. The substances used in the initial screening can be those that do not violate the Lipiskin law.[13]

In this section, we use virtual screeners Ghose, Veber, Egan, and Muegge to refine SC10, SC11, SC20, SC22, and SC26 compounds to have druglikeness properties.[14] This is a critical stage in the evaluation process that determines whether a compound is a potential drug compound. These

Table 2: The drug-like properties of the refined SC22 compound

Refined structure SC22		Druglike refined properties	
Virtual screening rules		Druglikeness properties	
Lipinski	Yes	Synthetic accessibility	4.11
Ghose	Yes	TPSA	45.29Å^2
Veber	Yes	Molar Refractivity	48.89
Egan	Yes	Num. rotatable bonds	3.0
Muegge	Yes	Log Po/w (MLOGP)	0.50

virtual screening rules will determine a druglikeness compound in a more comprehensive manner. The Ghose virtual screener specified druglikeness compounds with octanol-water distribution coefficients ranging from (-0.4) to (+0.56), molar refraction ranging from 40 to 130, and a total number of atoms ranging from 20 to 70. The Veber screener specifies a polarizing surface area of 140 Å^2 and a number of reducible bonds of 10. The substances with polar surface areas greater than 140 Å^2 will have difficulty passing through the cell membrane.

Compounds that pass through the blood-brain barrier must have a polar surface area of at least 90 Å^2. According to the Egan screener, a drug-like compound must have a topological polarization surface area (TPSA) of less than 131.1 Å^2 and logP < 5.88. The Muegge screener scores each molecule based on the presence of molecular structural fragments that are commonly found in drug molecules. When this score is between 2 and 7, molecules are classified as drugs. The virtual screening rules implemented also aid in determining the degree to which pharmacochemical synthesis can

be performed with values ranging from 1 to 10. The closer these values are to one, the easier it is to synthesize the compound. After passing through virtual screeners, we discovered that SC22 compound met the druglikeness requirements, as depicted in table 2.

The SC22 compound met the Lipinski rules and did not violate any of the drug-like properties conditions. The obtained drug-like properties of SC22 compound are all within the parameters of the Ghose, Veber, Egan, and Muegge rules. In addition, we also performed the determination of the molecular structure of SC22 by ^{1}H-NMR and ^{13}C-NMR nuclear magnetic resonance spectra in chloroform solvent, as demonstrated in figure 5. The properties of those spectra show that all of them give structural signals of the SC22 derivative present in *Cymbopogon citratus* volatile oil.

This is one in five structures with good inhibitory ability against SARS-CoV-2 effectively and has many druglikeness properties. this can be also a very important finding for a few chemical components of *Cymbopogon citratus* oil properties.
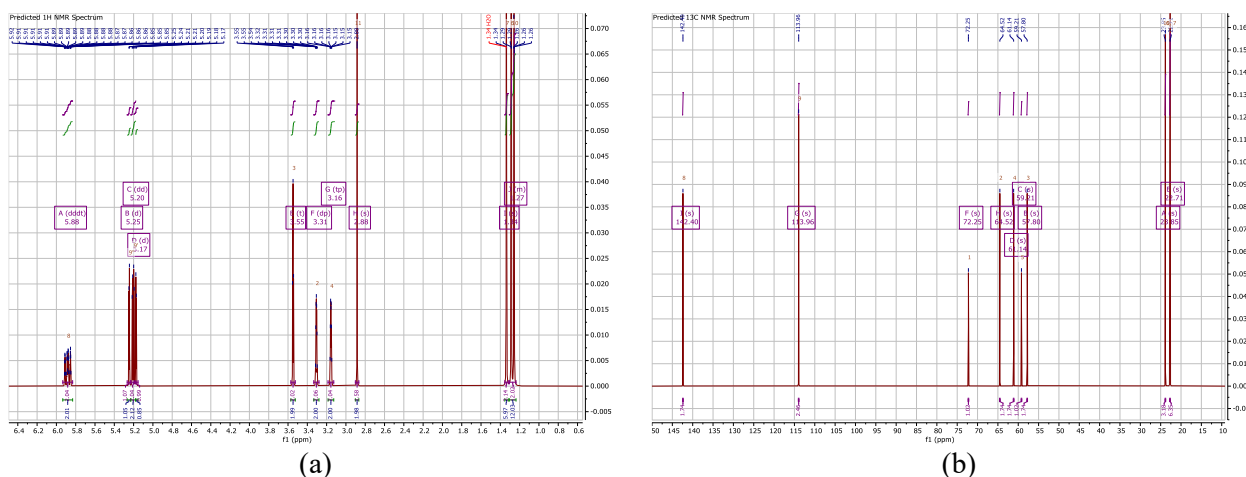
Figure 5: The structral spectra for SC22 compound: (a) ^{1}H-NMR, and (b) ^{13}C-NMR

This detected structure is in step with important measures of the activity and binding ability of the SC22 molecule to 6LU7 and ACE2. The 13C-NMR spectrum tells us the carbon structure style and carbon number through the height intensity shift. From this carbon skeleton structure, it's possible to grasp the connection between the structure and the activity of the compound.

The structural property that the H position in the OH group and near the -O- group has a binding activity to easily accept hydrogen is easily explained by the ^{1}H-NMR spectrum. The electron density in carbon atoms is high due to the action of the -CH$_3$ groups. The electrons at the carbon sites are located in the center of the molecule due to the influence of the ethylene oxide group. This structural site can also bind to the amino acids of the receptor site proteins 6LU7 and ACE2. This also makes hydrogen bond formation easier during docking and MD simulations. The ^{13}C-NMR spectrum demonstrates the full number of carbons in the molecular framework, with characteristic signals indicating the carbon number and chemical shift of the peaks on the spectrum, which is consistent with the nature and properties of the SC22 compound.

4. CONCLUSIONS

The simulation techniques demonstrated that 34 compounds in *Cymbopogon citratus* essential oil inhibit the proliferation ability of SARS-CoV-2; the docking model analysis for each ligand-protein complex demonstrated that the components of *Cymbopogon citratus* essential oil were effective.

The interaction distance and type of interaction revealed that substances in *Cymbopogon citratus* have ACE2 host receptor inhibitory activity as well as activity against the SARS-CoV-2 PDB6LU7 protein. Compound SC22 has the greatest inhibitory effect on both ACE2 and PDB6LU7 protein.

SC22, SC10, SC11, SC26, and SC20, with a total content of 49.25 percent, are five of the 34 substances in *Cymbopogon citratus* essential oil with the most potent inhibitory activity against the proteins ACE2 and PDB6LU7. In SARS-CoV-2, the potential drug-binding point for the ACE2 protein and the PDB6LU7 protein ranges from -7.98 to -13.3 kcal.mol^{-1}. The ligand-protein complex has an RMSD value less than 2.0 Å.

The molecular dynamics models of SC22-2CE2 and SC22-6LU7 compounds were satisfied with the docking simulation model. This study incorporates simulation techniques that allow the screening of applicable precursors to the development of new drugs.

We discovered the SC22 compound, which has many drug-like features and is easily synthesized, by applying virtual screening approaches based on Lipiski, Ghose, Veber, Egan, and Muegge criteria, as well as the refining technique to pick the compound with drug-like properties. This is the primary achievement of this work.

REFERENCES

1. S. Ahmad, Y. Waheed, S. Ismail, S. W. Abbasi, M. Hasan Najmi. A computational study to disclose potential drugs and vaccine ensemble for CoVID-19 conundrum, *J. Mol. Liq.*, **2020**, *324*, 114734.

2. S. Skariyachan, D. Gopal, S. Chakrabarti, P. Kempanna, A. Uttarkar, A. G. Muddebihalkar, V. Niranjan. Structural and molecular basis of the interaction mechanism of selected drugs towards multiple targets of SARS-CoV-2 by molecular docking and dynamic simulation studies- deciphering the scope of repurposed drugs, *Comput. Biol. Med.*, **2020**, *126*, 104054.

3. B. T. P. Thuy, T. T. A. My, N. T. T. Hai, L. T. Hieu, T. T. Hoa, H. T. P. Loan, N. T. Triet, T. T. V. Anh, P. T. Quy, P. V. Tat, N. V. Hue, D. T. Quang, N. T. Trung, V. T. Tung, H.K. Lam, and N. T. A. Nhung. Investigation into SARS-CoV-2 Resistance of Compounds in Garlic Essential Oil, *ACS Omega*, **2020**, *5(14)*, 8312.

4. T. T . A. My, H. T. P. Loan, N. T. T. Hai, L. T. Hieu, T. T. Hoa, B. T. P. Thuy, D. T. Quang, N. T. Triet, T. T. V. Anh, N. T. X. Dieu, N. T. Trung, N. V. Hue, P. V. Tat, V. T. Tung, N. T. A. Nhung. Evaluation of the Inhibitory Activities of CoVID-19 of *Melaleuca cajuputi* Oil Using Docking Simulation, *Chemistry Select*, **2020**, *5(21)*, 6312.

5. D. Shanmugarajan, P. Prabitha, B. R. P. Kumar, B. Suresh. Curcumin to inhibit binding of spike glycoprotein to ACE2 receptors: computational modelling, simulations, and ADMET studies to explore curcuminoids against novel SARS-CoV-2 targets, *RSC Advances*, **2020**, *10*, 31385.

6. S. A. Cherrak, H. Merzouk, N. Mokhtari-Soulimane. Potential bioactive glycosylated flavonoids as SARS-CoV-2 main protease inhibitors: A molecular docking and simulation studies, *PloS one*, **2020**, *15(10)*, 240653.

7. M. N. Boukhatem, M. A. Ferhat, A. Kameli, F. Saidi, H. T. Kebir. Lemon grass (Cymbopogon citratus) essential oil as a potent anti-inflammatory and antifungal drugs, *Libyan J. Medicine*, **2014**, *9*, 25431.

8. Y. Yang, M. S. Islam, J. Wang, Y. Li, X. Chen. Traditional Chinese Medicine in the Treatment of Patients Infected with 2019-New Coronavirus (SARS-CoV-2), *Int. J. Biol Sci*, **2020**, *16(10)*, 1708.

9. N. Jain, M. Sharma. Phytochemical Screening and

Antidermatophytic Activity of *Cymbopogon citratus* Leaves Essential Oil and their Fractions, *J. Essential Oil Bearing Plants*, **2017**, *20*(*4*), 1107.

10. 10. V. K. Bhari, D. Kumar, S. Kumar, R. Mishra. SARS-CoV-2 cell receptor gene ACE2-mediated immunomodulation in breast cancer subtypes, *Biochemistry and Biophysics Reports*, **2020**, *24*, 100844.

11. S. Keretsu, S. P. Bhujbal, S. J. Cho. Rational approach toward COVID-19 main protease inhibitors via molecular docking, molecular dynamics simulation and free energy calculation, *Scientific Reports,* **2020**, *10*(*1*), 17716.

12. T. Q. Bui, H. T. P. Loan, T. T. A. My, D. T. Quang, B. T. P. Thuy, V. D. Nhan, P. T. Quy, P. V. Tat, D. Q. Dao, N. T. Trung, H. K. Lam, N. T. A. Nhung. A density functional theory study on silver and bis-silver complexes with lighter tetrylene: are silver and bis-silver carbenes candidates for SARS-CoV-2 inhibition? Insight from molecular docking simulation, *RSC Advances*, **2020**, *10*, 30961.

13. C. A Lipinski, F. Lombardo, B. W. Dominy, P. J. Feeney. Experimental and computational approaches to estimate solubility and permeability in drug disCoVery and development settings, *Adv Drug Deliv Rev*, **2001**, *46*(*1*), 3.

14. A. B. Umar, A. Uzairu, G. A. Shallangwa, S. Uba. *In silico* evaluation of some 4-(quinolin-2-yl)pyrimidin-2-amine derivatives as potent V600E-BRAF inhibitors with pharmacokinetics ADMET and drug-likeness predictions, *Future Journal of Pharmaceutical Sciences,* **2020**, *6(61)*, 1.

Corresponding author: **Pham Van Tat**
Faculty of Health Sciences, Hoa Sen University
8 Nguyen Van Trang, District 1
Ho Chi Minh City 70000, Viet Nam
E-mail: vantat@gmail.com.